

Adsorbed Triblock Copolymers Deliver Reactive Iron Nanoparticles to the Oil/Water Interface

Navid Saleh,[†] Tanapon Phenrat,[†] Kevin Sirk,[‡] Bruno Dufour,[§] Jeongbin Ok,[§] Traian Sarbu,[§] Krzysztof Matyjaszewski,[§] Robert D. Tilton,^{‡,||} and Gregory V. Lowry^{*,†}

*Department of Civil & Environmental Engineering,
Department of Chemical Engineering, Department of Chemistry, and
Department of Biomedical Engineering, Carnegie Mellon University,
Pittsburgh, Pennsylvania 15213-3890*

Received September 12, 2005; Revised Manuscript Received October 31, 2005

ABSTRACT

Reactive zero valent iron nanoparticles can degrade toxic nonaqueous phase liquids (NAPL) rapidly in contaminated groundwater to nontoxic products in situ, provided they can be delivered preferentially to the NAPL/water (oil/water) interface. This study demonstrates the ability of novel triblock copolymers to modify the nanoiron surface chemistry in a way that both promotes their colloidal stability in aqueous suspension and drives their adsorption to the oil/water interface. The ability of the copolymers to drive adsorption is demonstrated by the ability of copolymer-modified iron nanoparticles, but not the unmodified iron nanoparticles, to stabilize oil-in-water emulsions.

Extensive efforts have been made in the past few decades to synthesize and characterize novel nanoparticles with unique reactivity and functions.¹ Engineering applications employing these novel nanomaterials have lagged their development because they are difficult to process. For example, they may not be readily dispersible in either aqueous or organic solvents or otherwise rapidly aggregate in suspension because of high surface energy and attractive van der Waals forces^{2,3} (e.g., carbon nanotubes are not readily dispersible in water⁴). Furthermore, it is difficult to deliver them to the specific regions where they are needed (e.g., for drug delivery⁵). To make use of the many types of nanoparticles that have been and will continue to be developed, methods are needed to prepare colloidally stable suspensions that are readily dispersible in the desired solvent and have the ability to target specific chemical environments where their actions are desirable. Recent advances in functionalizing the surfaces of iron-based nanoparticles are promising, and particles can now target cell-specific receptors such as glioma cells⁶ and can form stable colloidal suspensions in both organic and aqueous solvents.⁷ Polymer coatings are also used to provide the targeted delivery of drugs to specific receptors.⁸ Further, surface functionalization of nanoparticles

promotes their self-assembly at liquid–liquid interfaces^{9,10} (e.g., as in Pickering emulsions^{11,12}). Similar approaches can also benefit environmental applications of nanotechnology.

The remediation of chlorinated organic-contaminated groundwater using metallic or bimetallic reactive nanoparticles is one environmental nanotechnology application^{13–16} that could benefit from surface functionalization techniques. Groundwater contamination by chlorinated organic solvents (e.g., trichloroethene) is a particularly vexing and persistent environmental and human health concern.¹⁷ The contamination source is most often a chlorinated solvent that is present in the groundwater aquifer deep below the ground surface as a separate water-immiscible phase. This neat oil phase, commonly referred to as a nonaqueous phase liquid or NAPL, slowly dissolves and acts as a constant and very long-term (hundreds of years) groundwater contamination source. Conventional remediation methods (e.g., pump and treat or permeable reactive barriers¹⁸) and novel methods based on iron nanoparticle injection into aquifers¹⁵ address the dissolved contaminant plume and are not efficient. Directly attacking and removing the NAPL source is preferable.

To be effective for groundwater remediation, the iron nanoparticles not only must be dispersible in water under varying pH and ionic strength conditions and transportable through a water-saturated porous matrix but also must have an affinity for the NAPL/water interface such that the particles preferentially accumulate at this interface where they

* Corresponding author. E-mail: glowry@andrew.cmu.edu.

[†] Department of Civil & Environmental Engineering.

[‡] Department of Chemical Engineering.

[§] Department of Chemistry.

^{||} Department of Biomedical Engineering.

will degrade the NAPL most efficiently. Protecting nanoparticles from rapid flocculation using surfactant or polyelectrolyte coatings is a well-established technique.^{19,20} The coatings provide strong electrostatic and/or electrosteric repulsions that dominate over attractive van der Waals forces between particles.^{20,21} Because surfactant adsorption is readily reversible, it has limited applicability for environmental applications where injected nanoparticles must eventually be transported through surfactant-free water where the surfactant will desorb. In contrast, adsorption is essentially an irreversible process for high molecular weight polymers.^{22–24} Polymers can be grafted onto the particle surface via covalent bonds or physical adsorption onto the nanoparticle surfaces or polymers can be grafted from the particle surfaces.^{7,11,25–28} The former is a straightforward technique.²¹ The latter uses atom transfer radical polymerization (ATRP)^{29,30} to synthesize a very dense polymer brush layer from initiators that are covalently bound to the nanoparticle surfaces. Adsorbing or grafting polymers onto the nanoparticles is a less time- and material-intensive procedure than growing polymers from the particles and is desirable, especially if physical adsorption of polymers provides a surface coating with polymer densities sufficient for the intended task.

We describe here the preparation, characterization, and NAPL/water targeting ability of a novel organic–inorganic reactive nanoparticle system that forms colloiddally stable suspensions in water and whose amphiphilicity also provides the ability to target the NAPL/water interface. The effect of polymer architecture on colloidal stability in water is also presented. The hybrid nanoparticles are prepared using a multistep process where a commercially available reactive Fe⁰/Fe₃O₄ core–shell nanoparticle (Toda Kyogo, Japan) is modified with a novel triblock copolymer. The system is highly flexible such that metal oxide nanoparticles with different properties could also be used as the reactive core. The Fe⁰/Fe₃O₄ “reactive nanoiron particles” (RNIP) are synthesized from the reduction of Fe oxides to form Fe⁰, followed by partial oxidation through exposure to water to yield a stable Fe₃O₄ shell.³¹ The magnetite shell of the particle protects the Fe⁰ core from oxidizing too rapidly and provides a stable nonreactive surface that we use for subsequent modification. At ambient conditions in water, the Fe⁰ core is oxidized to Fe₃O₄ by the target contaminants such as trichloroethylene (TCE), which is reduced to nontoxic nonchlorinated products such as acetylene or ethane.¹⁴ In a 1 mM NaHCO₃ solution (pH = 7.4), the Fe⁰/Fe₃O₄ particles range in size from 100 to 200 nm as determined by dynamic light scattering (Figure 1) and have a measured electrophoretic mobility of $-2.3 \pm 0.15 \mu\text{mcm/Vs}$ (Table 1).

Design and ATRP Synthesis of Targeting Triblock Copolymers. Two polymer architectures were used (see Table 1, where subscripts denote block degrees of polymerization). The architecture of the poly(methacrylic acid)-*block*-poly(methyl methacrylate)-*block*-poly(styrenesulfonate) triblock copolymer (Figure 2) was designed to provide aqueous colloidal stability and sufficient amphiphilicity to anchor the particles at the NAPL/water interface. Polycarboxylic acids adsorb strongly to iron oxide surfaces.^{32–34}

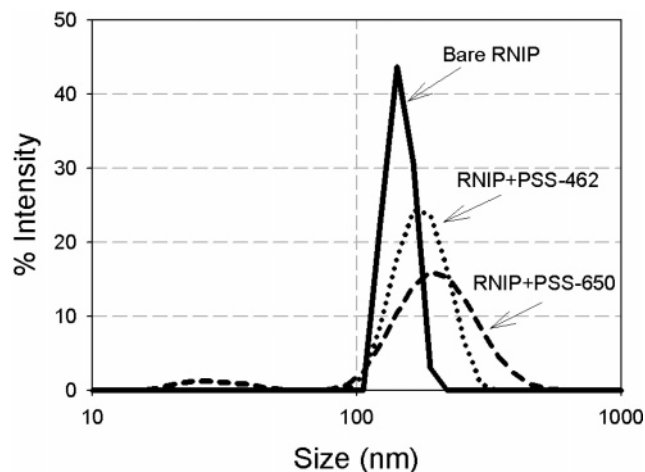


Figure 1. DLS intensity data for bare and modified iron nanoparticles.

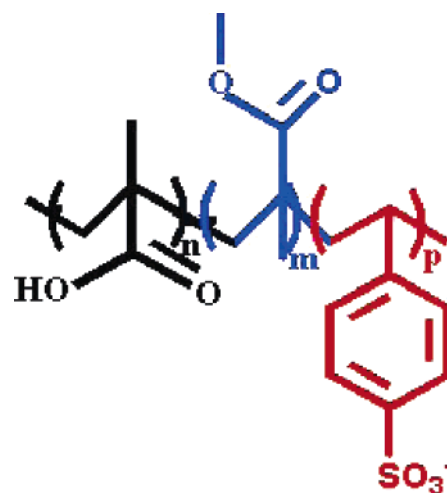


Figure 2. Hydrophobic–hydrophilic triblock copolymers containing a short PMAA anchoring group (left), PMMA hydrophobic block (middle), and a hydrophilic sulfonated polystyrene block (right).

Table 1. Polymer Properties and Mean DLS Particle Sizes and Electrophoretic Mobility Measured in a 1 mM NaHCO₃ Solution (pH = 7.4)

polymeric surface modification	M_n^a (PDI ^b)	mean diameter (nm)	electrophoretic mobility ($\mu\text{mcm/Vs}$)
none		146 ± 4	-2.3 ± 0.15
PMAA ₄₂ -PMMA ₂₆ -PSS ₄₆₂	56 100 (1.24)	178 ± 11	-3.82 ± 0.16
PMAA ₄₈ -PMMA ₁₇ -PSS ₆₅₀	75 600 (1.62)	212 ± 21	-3.14 ± 0.07

^a Measured before sulfonation. ^b Polydispersity index.

Thus, the poly(methacrylic acid) (PMAA) block serves to anchor the triblock copolymers to the magnetite shell. Hydrophobic attractions arising from the poly(methyl methacrylate) (PMMA) block provide the strong affinity to the NAPL and create a low polarity region that hinders water access to the RNIP with the goal of minimizing iron nanoparticle oxidation during transport in the soil before it

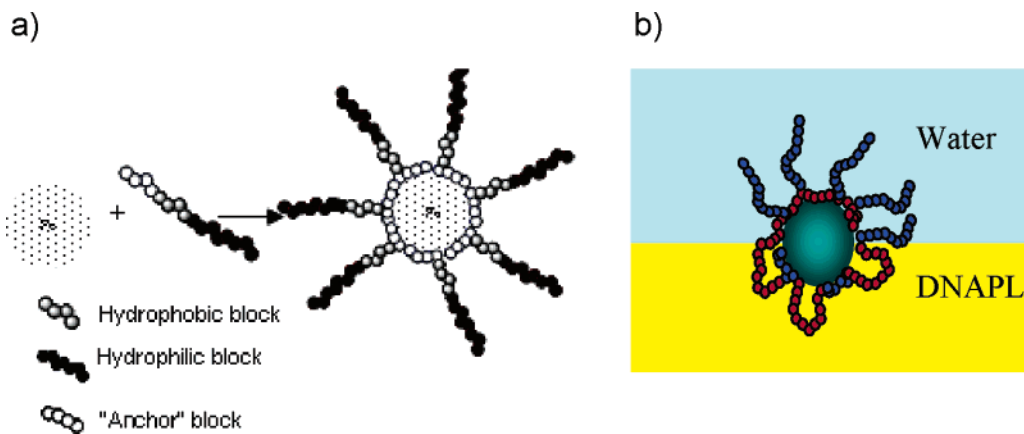


Figure 3. (a) Polyelectrolyte modified iron nanoparticles and (b) proposed polymer layer response at DNAPL/water interface.

reaches the NAPL. (The barrier properties of this block have not yet been investigated.) The strong polyanion poly(styrenesulfonate) (PSS) block serves to provide strong electrosteric interparticle repulsions that promote colloidal stability and electrosteric repulsion from the negatively charged surfaces (e.g., Fe and Mn oxides, natural organic matter) that are predominant in the subsurface at near neutral pH. The functioning of this triblock copolymer is illustrated schematically in Figure 3. In water, the PMMA block is collapsed, while the extended PSS block provides electrosteric protection. At the NAPL/water interface, the PMMA block swells in the organic solvent and anchors the particle at the interface. PSS solubility in the organic phase is too weak to allow full passage of the nanoparticle through the interface into the bulk NAPL phase.

The designed triblock copolymers were prepared using the general method developed by Ok and co-workers (2005).³⁵ First, a triblock copolymer [poly(*tert*-butyl methacrylate)]-[poly(methyl methacrylate)]-[polystyrene] was synthesized by atom transfer radical polymerization (ATRP).³⁰ The preparation is described in the Supporting Information. The molecular weight and polydispersity index (PDI) of the final triblock copolymer and of each intermediate (co)-polymer were analyzed by gel permeation chromatography (GPC) and are also provided in the Supporting Information. The PDI of each triblock copolymer was between 1.2 and 1.6 (Table 1). This polymer was then converted to [poly(methacrylic acid)]-[poly(methyl methacrylate)]-[poly(styrenesulfonate)] via simultaneous hydrolysis of the *tert*-butyl group and sulfonation of polystyrene using acetyl sulfate, which allows a high degree of modification.³⁶

The triblock copolymers are physisorbed to the surfaces of the Fe⁰/Fe₃O₄ nanoparticles by adding an aqueous slurry of nanoparticles to a 2 g/L polymer solution containing 1 mM NaHCO₃ as the background electrolyte (pH = 7.4). The mixture is sonicated using an ultrasonic probe for 30 min followed by gentle end-over-end rotation for 72 h. The suspensions are then centrifuged and washed multiple times to remove any excess nonadsorbed polymer from the system. The same procedure was used for control experiments using PSS poly(sodium 4-styrenesulfonate) homopolymer (Aldrich) with degrees of polymerization of 340 and 970 or with a

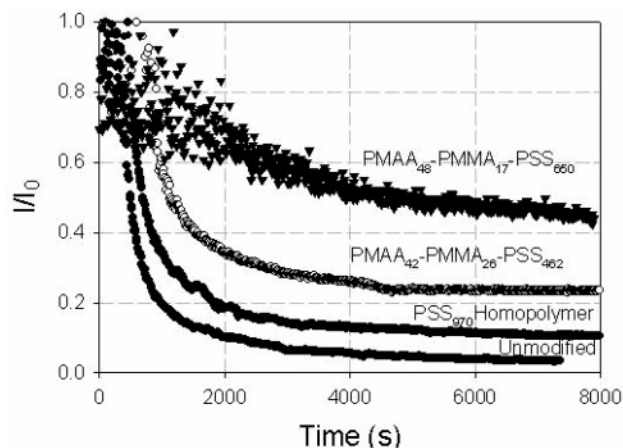


Figure 4. Sedimentation curves for bare and modified iron nanoparticle dispersions (0.08 wt %) in water. The PSS₃₄₀ homopolymer and the PBMA₄₃-PSS₈₁₁ diblock lie between the PSS₉₇₀ homopolymer and PMAA₄₂-PMMA₂₆-PSS₄₆₂ and are not shown for clarity.

poly(butyl methacrylate)-*block*-poly(styrene sulfonate) diblock copolymer (PBMA₄₃-PSS₈₁₁) that omitted the PMAA block.

The sizes and electrophoretic mobilities of bare and polymer-modified particles were measured in dilute (10⁻³ wt %) suspensions using a Malvern Zetasizer Nano ZS (Table 1). The size distribution is reported as the distribution of hydrodynamic diameters, assuming spherical particles. The colloidal stability of the nanoparticles was determined by measuring the sedimentation rate of the nanoparticle suspensions (Figure 4). The optical density ($\lambda = 508$ nm) of 0.08 wt % suspensions was monitored for 2.5 h in a UV-vis spectrophotometer. The dispersions were shaken gently by hand immediately prior to the flocculation/sedimentation measurements.

Nanoparticle Size Distribution. Unmodified RNIP suspensions are polydisperse, with particle diameters in the 100–200-nm size range. This is 2–10 times larger than the primary particle size of RNIP observed by TEM.^{14,37} It is possible that preexisting aggregates were not completely dispersed during sonication. The average hydrodynamic diameter of polymer-modified RNIP increases by approximately 30–50 nm, an increment that is consistent with the expected brush thickness for the triblock copolymers having

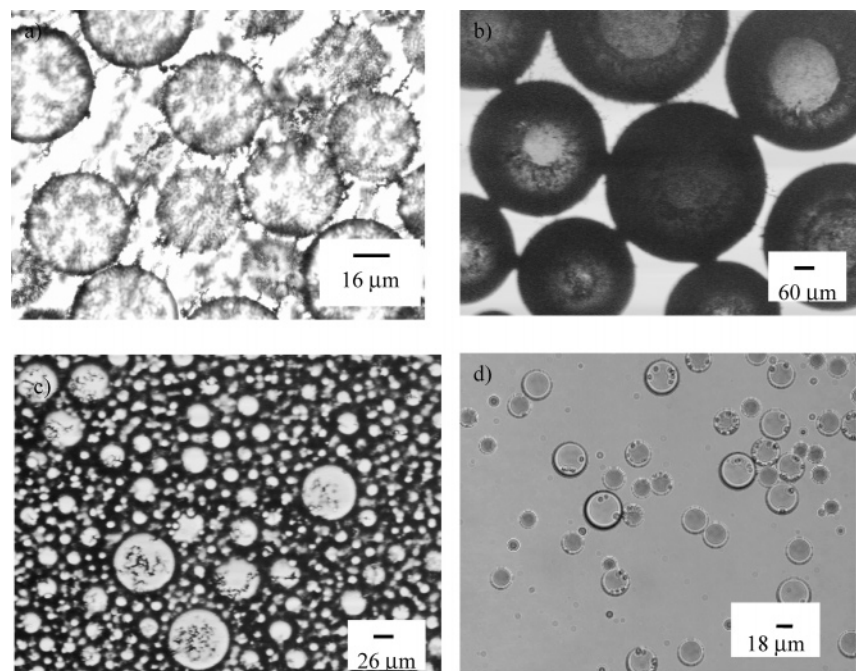


Figure 5. Micrographs of emulsified TCE (a–b) and dodecane (c) droplets in water stabilized by raw PMAA₄₂–PMMA₂₆–PSS₄₆₂ triblock copolymer-modified iron nanoparticles and TCE (d) by fractionated PMAA₄₂–PMMA₂₆–PSS₄₆₂ triblock copolymer-modified iron nanoparticles.

the PSS degrees of polymerization used here.³⁸ Sample polydispersity precludes a definitive determination of the polymer layer thickness. The small scattering peak in the 10–30-nm range appeared only for the PMAA₄₈–PMMA₁₇–PSS₆₅₀-modified samples (Figure 1). It matches the size measured in particle-free solutions of this polymer, suggesting that nonadsorbed polymer removal from this sample was incomplete.

Effect of Polymer Coatings on Electrophoretic Mobility and Colloidal Stability. Without surface modification, RNIP particles rapidly flocculate and sediment from solution (Figure 4) because of strong short-range van der Waals interactions and other long-range forces attributable to the magnetic properties of Fe₃O₄.³⁹ Modification by each polymer increased the electrophoretic mobility of the particles (Table 1) and increased the stability of the suspensions relative to bare RNIP significantly (Figure 4). The suspension stability increased as the PSS block degree of polymerization increased from 462 to 650, without a corresponding increase in the electrophoretic mobility. Thus, the larger PSS block of PMAA₄₈–PMMA₁₇–PSS₆₅₀ provided stronger electrosteric repulsions and better stability improvement than PMAA₄₂–PMMA₂₆–PSS₄₆₂, as would be expected for these polymers that are otherwise quite similar to each other.^{40,41} Particles modified with PSS homopolymers or with PBMA₄₃–PSS₈₁₁ were more stable than bare RNIP, but less stable than the triblock copolymers (Figure 4). This indicates that PSS homopolymers and the diblock do adsorb to RNIP to some degree but in a configuration that is less effective for colloidal stabilization than the triblock copolymers that contain the PMAA anchor block.

NAPL/Water Interfacial Targeting. In addition to improving RNIP colloidal stability, these amphiphilic copoly-

mers also drive RNIP adsorption to the NAPL/water interface. This was demonstrated by emulsification experiments, following procedures described by Saleh and co-workers for preparing Pickering emulsions with PSS-modified silica nanoparticles.¹¹ TCE, a DNAPL (denser than water nonaqueous phase liquid), and dodecane, a LNAPL (lighter than water nonaqueous phase liquid) were emulsified in the presence of polymer-modified RNIP particle suspensions. Successful emulsification was achieved using either “raw” polymer-modified RNIP suspensions that included both the stably suspended particles and the larger aggregates that would ordinarily sediment rapidly, as well as “fractionated” suspensions containing only the most highly stable suspension that remained over a sedimented particle bed (Figure 5). Both polymers were effective surface modifiers. Extremely stable oil-in-water Pickering emulsions were formed with the polymer-coated RNIP suspensions. Emulsions prepared with RNIP coated by adsorbed PMAA₄₂–PMMA₂₆–PSS₄₆₂ have been stable for over six months. The presence of an oil-in-water emulsion was verified by the drop test, that is, a drop of emulsion sample readily mixed with excess water and was therefore not oil-continuous. The black appearance of the emulsion phase and the clarity of the excess water phase made it apparent that the emulsion contained nearly all of the RNIP. The equal emulsification effectiveness of raw and fractionated polymer-modified RNIP suspensions indicates that particle preflocculation is not the critical factor in the emulsion stability for this system.⁴² To verify that emulsification was due to particle adsorption rather than free polymer adsorption, we ran emulsification experiments with the supernatant of a polymer-modified RNIP sample that had been ultracentrifuged. This supernatant, which would contain the free polymer that would have

coexisted with the RNIP suspension, produced no emulsification. Thus, these are true Pickering emulsions, stabilized by particle adsorption at the oil–water interface. Control experiments using bare RNIP or RNIP modified with PSS homopolymers or with a PBMA₄₃–PSS₈₁₁ diblock copolymer (i.e., no PMAA) did not form an emulsion phase, indicating that the adsorbed triblock copolymers and the specific triblock architecture used were essential for RNIP adsorption to the oil–water interface.

Emulsions prepared with 0.3 wt % suspensions of PMAA₄₂–PMMA₂₆–PSS₄₆₂ triblock-modified RNIP contained a bimodal distribution of stable TCE-in-water emulsion droplets. Most droplets ranged from 32 to 44 μm in diameter (Figure 5a), but a smaller number of larger droplets with diameters of 440–500 μm (Figure 5b) coexisted with the smaller droplets. Under the same conditions, emulsified dodecane droplets ranged in size from 5 to 50 μm , indicating that the properties of the NAPL phase affect the emulsion droplet size (Figure 5c). The emulsion droplets formed using the fractionated polymer-modified RNIP suspension had smaller diameters, ranging from 5 to 20 μm (Figure 5d). The narrow size distribution of emulsion droplets is typical of stable Pickering emulsions.¹¹

Figure 5a shows that a distinct shell of aggregated iron nanoparticles surrounds the TCE droplets. The flocculated particles surrounding the emulsion droplets appear to form dendritic structures, and the emulsion droplets are held apart by these aggregates of particles. The reasons for the formation of the dendritic structures are not firmly established but may be due to strong particle–particle affinity because of their high Hamaker constant, bridging by the polymer chains, or long-range magnetic attractions between the particles.^{43,44} The width of the aggregated nanoiron shells around the droplets is approximately 1 μm , indicating that they are approximately 5–10 particles thick. Nanoiron was not found inside the emulsion droplets, which is consistent with the facts that the emulsion was of the oil-in-water type and that the polymer-coated nanoparticles are not dispersible in pure TCE or dodecane. The ability of these particles to form a highly stable emulsion phase demonstrates the ability of amphiphilic triblock copolymer modified iron nanoparticles to preferentially localize at the oil (DNAPL or LNAPL)/water interface.

Physisorbed layers of amphiphilic PMAA-*block*-PMMA-*block*-PSS triblock copolymers improve the colloidal stability of Fe⁰/Fe₃O₄ nanoparticles in water and drive them to adsorb at the oil/water interface. This satisfies two requirements for the development of a polymeric targeted reactive nanoiron delivery system for the remediation of chlorinated solvent-contaminated groundwater. The effect of these triblock copolymers on nanoparticle transport through model saturated sand columns will be described elsewhere.⁴⁵ The flexibility of the triblock copolymer synthesis enables systematic variations in polymer architecture in order to engineer the dispersion stability and targeting properties of nanoiron suspensions for different application environments.

Acknowledgment. This research was funded by the Office of Science (BER), U.S. Department of Energy, grant

no. DE-FG07-02ER63507, the U.S. EPA (R830898), and the NSF (CTS-0521721). Although the research described in this paper has been funded by the United States Environmental Protection Agency, it has not been subjected to the Agency's required peer and policy review and therefore does not necessarily reflect the views of the Agency, and no official endorsement should be inferred. Any opinions, findings, and conclusions or recommendations expressed in this material are those of the authors and do not necessarily reflect the views of the Department of Energy. We thank all of the project team at CMU for insightful and helpful discussions.

Supporting Information Available: Description of the polymer synthesis using ATRP and the emulsion preparation and stability for copolymers and homopolymers. This material is available free of charge via the Internet at <http://pubs.acs.org>.

References

- (1) Li, X. G.; Takahashi, S.; Watanabe, K.; Kikuchi, Y.; Koishi, M. *Nano Lett.* **2001**, *1*, 475–480.
- (2) Hiemenz, P. C.; Rajagopalan, R. *Principles of Colloid and Surface Chemistry*, 3rd ed.; Marcel Dekker: New York, 1997.
- (3) Schrick, B.; Hydutsky, B.; Blough, J.; Mallouk, T. *Chem. Mater.* **2004**, *16*, 2187–2193.
- (4) Sayes, C. M.; Fortner, J. D.; Guo, W.; Lyon, D.; Boyd, A. M.; Ausman, K. D.; Tao, Y. J.; Sitharaman, B.; Wilson, L. J.; Hughes, J. B.; West, J. L.; Colvin, V. L. *Nano Lett.* **2004**, *4*, 1881–1887.
- (5) Barauskas, J.; Johnsson, M.; Tiberg, F. *Nano Lett.* **2005**, *5*, 1615–1619.
- (6) Veiseh, O.; Sun, C.; Gunn, J.; Kohler, N.; Gabikian, P.; Lee, D.; Bhattarai, N.; Ellenbogen, R.; Sze, R.; Hallahan, A.; Olson, J.; Zhang, M. *Nano Lett.* **2005**, *5*, 1003–1008.
- (7) Duan, H.; Kuang, M.; Wand, D.; Kurth, D. G.; Mohwald, H. *Angew. Chem.* **2005**, *44*, 1717–1720.
- (8) Chen, C.-C.; Dormidontova, E. E. *Langmuir* **2005**, *21*, 5605–5615.
- (9) Lin, Y.; Skaff, H.; Emrick, T.; Dinsmore, D.; Russell, T. P. *Science* **2003**, *299*, 226–229.
- (10) Duan, H.; Wang, D.; Kurth, D. G.; Mohwald, H. *Angew. Chem. Int. Ed.* **2004**, *43*, 5639–5642.
- (11) Saleh, N.; Sarbu, T.; Sirk, K.; Lowry, G. V.; Matyjaszewski, K.; Tilton, R. D. *Langmuir* **2005**, *21*, 9873–9878.
- (12) Dai, L.; Sharma, R.; Wu, C. *Langmuir* **2005**, *21*, 2641–2643.
- (13) Liu, Y.; Choi, H.; Dionysiou, D.; Lowry, G. V. *Chem. Mater.* **2005**, *17*, 5315–5322.
- (14) Liu, Y.; Majetich, S. A.; Tilton, R. D.; Sholl, D. S.; Lowry, G. V. *Environ. Sci. Technol.* **2005**, *39*, 1338–1345.
- (15) Elliott, D. W.; Zhang, W. *Environ. Sci. Technol.* **2001**, *35*, 4922–4926.
- (16) Rabelo, D.; Lima, E. C. D.; Reis, A. C.; Nunes, W. C.; Novak, M. A.; Garg, V. K.; Oliveria, A. C.; Morais, P. C. *Nano Lett.* **2001**, *105*–108.
- (17) NRC *Contaminants in the Subsurface: Source Zone Assessment and Remediation*; National Academies Press: Washington, D.C., 2004.
- (18) LaGrega, M.; Buckingham, P.; Evans, J. *Hazardous Waste Management*, 2nd ed.; McGraw-Hill: Boston, MA, 2001.
- (19) Rosen, M. J. *Surfactants and Interfacial Phenomena*, 3rd ed.; Wiley-Interscience: New York, 2002.
- (20) Pincus, P. *Macromolecules* **1991**, *24*, 2912–2919.
- (21) Romet-Lemonne, G.; Guenoun, D.; Yang, J.; Mays, J. *Phys. Rev. Lett.* **2004**, *93*, 148301_148301–148301_148304.
- (22) Braem, A. D.; Biggs, S.; Prieve, D. C.; Tilton, R. D. *Langmuir* **2003**, *19*, 2736–2744.
- (23) Holmberg, K.; Jönsson, B.; Kronberg, B.; Lindman, B. *Surfactants and Polymers in Aqueous Solution*, 2nd ed.; John Wiley & Sons: West Sussex, U.K., 2003.
- (24) Velegol, S. B.; Tilton, R. D. *Langmuir* **2001**, *17*, 219–227.
- (25) Marutani, E.; Yamamoto, S.; Ninjbadgar, T.; Tsujii, Y.; Fukuda, T.; Takano, M. *Polymer* **2004**, *45*, 2231–2235.
- (26) Yoshikawa, C.; Goto, A.; Tsujii, Y.; Fukuda, T.; Yamamoto, K.; Kishida, A. *Macromolecules* **2005**, *38*, 4604–4610.

- (27) Pyun, J.; Kowalewski, T.; Matyjaszewski, K. *Macromol. Rapid Commun.* **2003**, *24*, 1043–1059.
- (28) Matyjaszewski, K.; Miller, P. J.; Shukla, N.; Immaraporn, B.; Gelman, A.; Luokala, B. B.; Siclovan, T. M.; Kickelbick, G.; Vallant, T.; Hoffmann, H.; Pakula, T. *Macromolecules* **1999**, *32*, 8716–8724.
- (29) Matyjaszewski, K.; Xia, J. *Chem. Rev.* **2001**, *101*, 2921–2990.
- (30) Davis, K. A.; Matyjaszewski, K. *Adv. Polym. Sci.* **2002**, *159*, 2–166.
- (31) Uegami, M.; Kawano, J.; Okita, T.; Fujii, Y.; Okinaka, K.; Kakuya, K.; Yatagai, S. U.S. Patent 20030217974A1, 2003.
- (32) Nakamae, K.; Tanigawa, S.; Nakano, S.; Sumiya, K. *Colloids Surf.* **1989**, *37*, 379–386.
- (33) Chibowski, S.; Wisniewska, M. *Colloids Surf., A* **2002**, *208*, 131–145.
- (34) Drzymala, J.; Fuerstenau, D. W. *Pol. Process Technol. Proc.* **1987**, *4*, 45–60.
- (35) Ok, J.; Dufour, B.; Sarbu, T.; Matyjaszewski, K. Abstracts of Papers, 230th ACS National Meeting, Washington, DC, Aug 28–Sept 1, 2005, POLY-479.
- (36) Thaler, W. A. *Macromolecules* **1983**, *16*, 623–628.
- (37) Nurmi, J. T.; Tratnyek, P. G.; Sarathy, V.; Baer, D. R.; Amonette, J. E.; Pecher, K.; Wang, C.; Linehan, J. C.; Matson, D. W.; Penn, R. L.; Driessen, M. D. *Environ. Sci. Technol.* **2005**, *39*, 1221–1230.
- (38) Zhulina, E. B.; Borisov, O. V.; Birshtein, T. M. *J. Phys. II France* **1992**, *2*, 63–74.
- (39) Donselaar, L. N.; Philipse, A. P. *J. Colloid Interface Sci.* **1999**, *212*, 14–23.
- (40) Morrison, I. D.; Ross, S. *Colloidal Dispersions: Suspensions, Emulsions, and Foams*; Wiley-Interscience: New York, 2002.
- (41) Tamashiro, M. N.; Hernandez-Zapata, E.; Schorr, P. A.; Balastre, M.; Tirrell, M.; Pincus, P. *J. Chem. Phys.* **2001**, *115*, 1960–1969.
- (42) Midmore, B. R. *Colloids Surf., A* **1998**, *132*, 257–265.
- (43) Xu, A.; Cai, P.; Ye, Q.; Xia, A.; Ye, G. *Phys. Lett. A* **2005**, *338*, 1–7.
- (44) Zhang, L.; Manthiram, A. *Appl. Phys. Lett.* **1997**, *70*, 2469–2471.
- (45) Saleh, N.; Sirk, K.; Dufour, B.; Matyjaszewski, K.; Tilton, R. D.; Lowry, G. V., in preparation.

NL0518268